Fermilab

Fermi National Accelerator Laboratory
P.O. Box 500 • Batavia, Illinois • 60510

TD-97-039
September 10, 1997

Calculation of Integrated Multipole Field Components in the HGQ End Regions

G. Sabbi

Abstract:
In this note the integrated multipole field components of the HGQ lead and return ends calculated using ROXIE are presented and compared with the results of previous calculations carried out using FIGENDS.

1 Introduction

In order to carry out precise calculations of field quality in the HGQ [1] end regions, which have been mechanically optimized using BEND [2], a new interface between BEND [3] and ROXIE [4] has been developed. The results obtained with the new code for the integrated multipole field components of the HGQ lead and return ends are here presented and compared with those obtained using FIGENDS [5].

2 Field representation

In the straight section of the magnet, where translational symmetry applies and the longitudinal component of the magnetic field vanishes, the field quality can be described in terms of multipole coefficients defined according to the following expression:

$$B_y + iB_x = \sum_{n=1}^{\infty}(B_n + iA_n)\left(\frac{x+iy}{r_0}\right)^{n-1} \tag{1}$$

Here a reference radius r_0 of 1 cm is chosen. The B_n and A_n parameters are usually referred to as normal and skew harmonic coefficients. For a quadrupole magnet, it is often convenient to express the multipole components in "units" of 10^{-4} of the main quadrupole field B_2:

$$b_n = B_n/B_2 \cdot 10^4 \tag{2}$$
$$a_n = A_n/B_2 \cdot 10^4 \tag{3}$$

For the (z-dependent) transverse field in the end regions of the magnet, one can retain the multipole expansion (1) as in the straight section, but apply it directly to the integrated field instead than to the local field:

$$\int_{z_p}^{z_q} (B_y + iB_x) dz = \sum_{n=1}^{\infty} (\hat{B}_n{}^{[z_p,z_q]} + i\hat{A}_n{}^{[z_p,z_q]}) \left(\frac{x+iy}{r_0} \right)^{n-1} \tag{4}$$

In analogy to 2, 3, the integrated multipole components can be expressed in "units" of 10^{-4} of the main integrated quadrupole field $\hat{B}_2^{[z_p,z_q]}$:

$$\hat{b}_n^{[z_p,z_q]} = \frac{\hat{B}_n^{[z_p,z_q]}}{\hat{B}_2^{[z_p,z_q]}} \cdot 10^4 \tag{5}$$

$$\hat{a}_n^{[z_p,z_q]} = \frac{\hat{A}_n^{[z_p,z_q]}}{\hat{B}_2^{[z_p,z_q]}} \cdot 10^4 \tag{6}$$

$$\tag{7}$$

The integrated multipole components in the interval $[z_p, z_q]$ can be related to the multipole field components in the straight section if the magnetic length of the interval $[z_p, z_q]$ is known:

$$L_m^{[z_p,z_q]} = \frac{\hat{B}_2^{[z_p,z_q]}}{B_2} \tag{8}$$

3 End Geometry

The longitudinal cross-sections of the HGQ return and lead end at the pole plane are shown in figure 1 and 2. In each case, the origin of the z-axis is chosen as defined in [2]. The z-axis is directed outwards from the magnet body. The iron yoke starts at z=-15 cm for the lead end, at z=-5 cm for the return end. In the lead end, the splice ramp starts at z=-13.78 cm for both the inner and the outer coil.

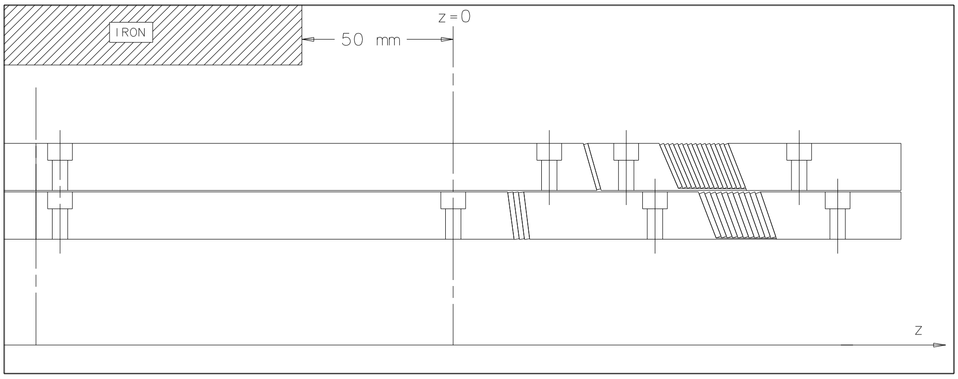

Figure 1: HGQ return end geometry

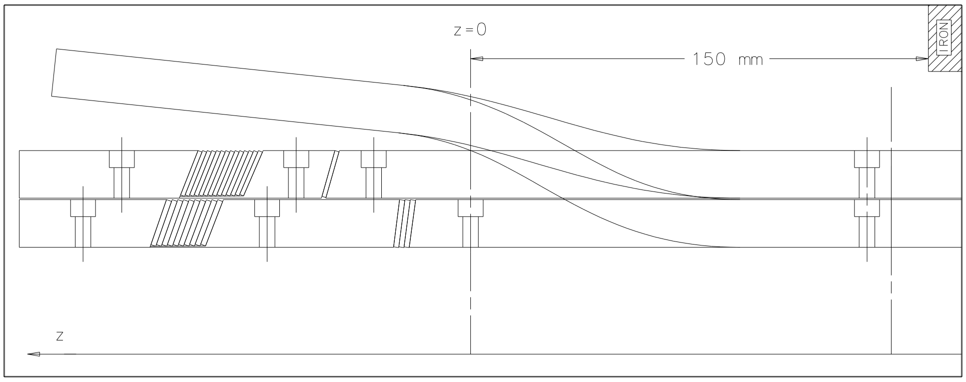

Figure 2: HGQ lead end geometry

4 Magnet model

The computer model for the end regions is created by reading into the ROXIE program the BEND coordinates files which specify the cross-sections of each conductor at small intervals along z. This is achieved by pre-processing the BEND coordinate files with the interface program BENDRX. The geometry of the lead end conductors has been specified using 30 cross-sections from the edge of the iron yoke outwards, while for the return end only 20 cross-sections have been used. The resulting geometry is shown in figure 3 and 4. The quadrant splices are not included in the model; for each coil, the two connection conductors extend straight from the magnet body in the z direction and are truncated at z=15 cm. The coil to coil splice length is 11.43 cm.

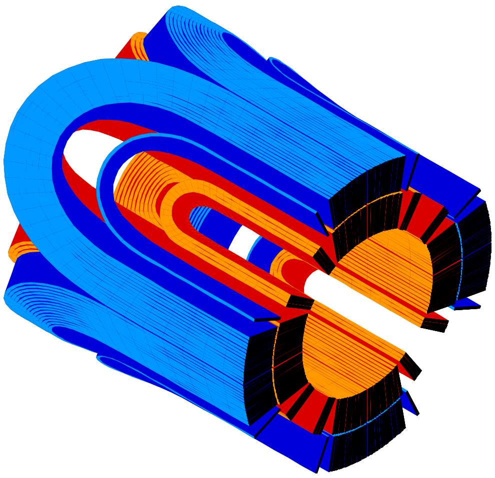

Figure 3: ROXIE-BEND model for the HGQ return end. Only the part of the coil extending beyond the edge of the iron yoke is shown. The model also includes a straight section extending from the edge of the iron yoke for 1.5 m in the negative z direction.

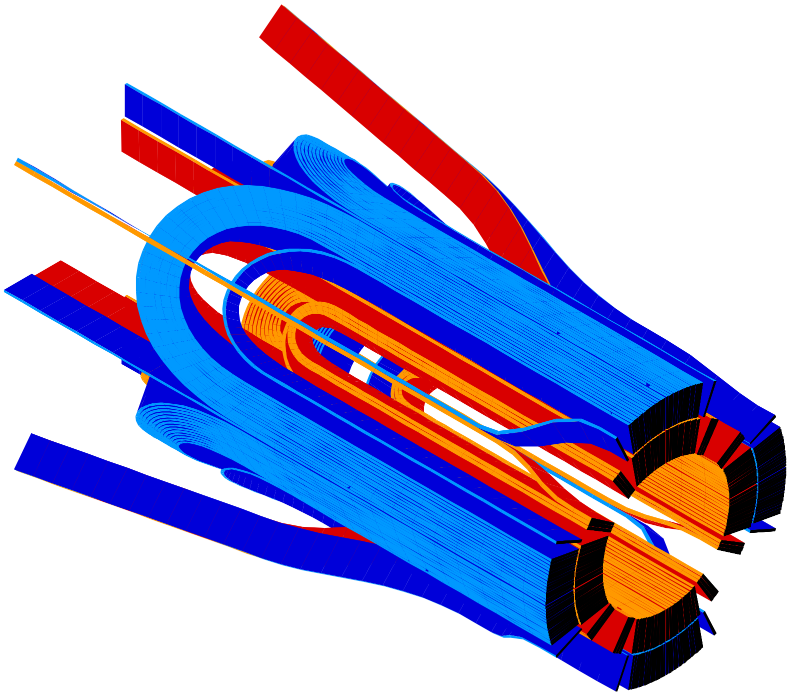

Figure 4: ROXIE-BEND model for the HGQ lead end. Only the part of the coil extending beyond the edge of the iron yoke is shown. The model also includes a straight section extending from the edge of the iron yoke for 1.5 m in the negative z direction.

The field calculation is based on the Biot-Savart law. The iron yoke is regarded as a magnetic mirror of circular shape (inner radius 9.256 cm) with infinite permeability. For the ROXIE calculation, each conductor has been subdivided in current filaments, one for each strand. The total number of strands is 38 in the inner layer, 46 in the outer layer. For both the lead and the return end calculations, a straight section extending in the negative z direction for 1.5 m from the start of the iron yoke towards the magnet body has been assumed.

5 Integrated multipole components

The ROXIE integrated multipole components have been obtained from 50 line integrals of the transverse field components, calculated along lines parallel to the z-axis, at the reference radius of 1 cm and equally spaced azimuthal angles. In order to carry out a consistent comparison with FIGENDS, the same integration limits as in [5] have been chosen: [-24,+20] cm for the lead end and [-14,+20] cm for the return end. Each field integral has been evaluated by adding up the contributions calculated at 0.2 cm intervals along z. The results for the magnetic length and the integrated multipole components in the HGQ return and lead end are reported in table 1 and 2.

Parameter	ROXIE	FIGENDS	Δ_{FR}
L_m (cm)	20.86	20.86	0.0
$\hat{b}_2$	10000	10000	
$\hat{b}_6$	0.082	0.129	0.047
$\hat{b}_{10}$	-0.00626	-0.00617	0.00009
$\hat{b}_{14}$	-0.000018		

Table 1: Integrated harmonic coefficients for the HGQ return end. The integration interval starts at z=-14 cm and ends at z=+20 cm.

Parameter	ROXIE	FIGENDS	Δ_{FR}
L_m (cm)	29.79	29.47	-0.32
$\hat{b}_2$	10000	10000	
$\hat{b}_6$	0.82	0.67	-0.15
$\hat{b}_{10}$	-0.00447	-0.00512	-0.00065
$\hat{b}_{14}$	-0.000014		
$\hat{a}_2$	58.56	61.46	2.9
$\hat{a}_6$	0.034	-0.051	-0.085
$\hat{a}_{10}$	-0.00149	-0.00148	0.00001
$\hat{a}_{14}$	0.000009		

Table 2: Integrated harmonic coefficients for the HGQ lead end. The integration interval starts at z=-24 cm and ends at z=+20 cm.

A good agreement between the results of ROXIE and FIGENDS is observed for most quantities; in some cases, however, discrepancies are observed, which require further investigation. In particular, the result from ROXIE for the gradient transfer function for the body of the magnet (z=-45 cm) is 18.22 T/m/kA, while the FIGENDS result is 0.1851 T/m/kA. This may depend on how the current density is distributed in the cable cross-section.

For what concerns the magnetic length, the results for the return end are identical, while in the lead lend a difference of 0.3 cm is found. This may be partly explained by differences in the model geometry, since the length of the leads and the length of the coil splice are not specified in the BEND coordinate files.

For what concerns the integrated multipoles, it should be noted that in some cases the integral is obtained as sum of local contributions of opposite sign, as shown in figure 5, where the normal dodecapole density function $\bar{b}_6(z)$ is plotted as function of z. This situation tends to amplify the dependence of the results on the choice of parameters like the number of current filaments, the length of the integration steps, the number of conductor cross-sections used to describe the end geometry.

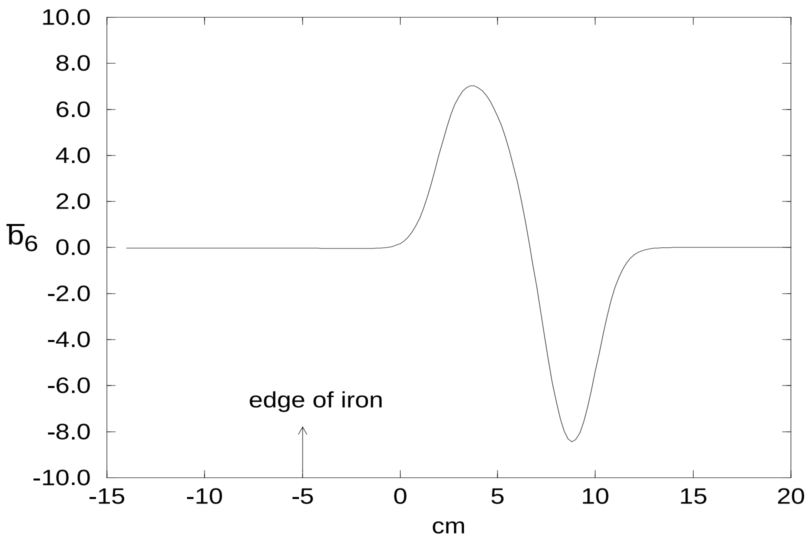

Figure 5: Normal dodecapole as function of z in the HGQ return end.

The multipole density function is defined as follows:

$$\bar{b}_n(z) = \lim_{\Delta \to 0} \frac{1}{\Delta} \hat{b}_n^{[z,z+\Delta]} \tag{9}$$

The result presented in figure 5 has been obtained using an integration interval Δ=0.2 cm.

References

[1] R. Bossert et al., *"Development of a High Gradient Quadrupole for the LHC Interaction Regions"*, ASC '96, Pittsburgh, August 1996.

[2] J. Brandt, A, Simmons, *"Coil End Design for the LHC IR Quadrupole Magnet"*, Fermilab TS-96-013, November 1996.

[3] J. Cook, *"Strain Energy Minimization in SSC Magnet Winding"*, IEEE Transactions on Magnetics, vol. 27, pp. 1976-1980, March 1991.

[4] S. Russenschuck, *"A computer program for the design of superconducting accelerator magnets"*, Proc. ACES Symposium, Monterey, California, 1995 and CERN AT/95-39, September 1995.

[5] S. Caspi, K. Chow, *"Normal and Skew Multipoles in the LHC Low Beta Quad - Rev. 1"*, LBL SC-MAG-577, February 1997.